THE JOURNAL OF CHEMICAL PHYSICS **128**, 164715 (2008)

The effect of fullerene derivative on polaronic charge transfer in poly(3-hexylthiophene)/fullerene compound

V. I. Krinichnyi,[a] P. A. Troshin, and N. N. Denisov
Institute of Problems of Chemical Physics, Semenov Avenue 1, Chernogolovka 142432, Russia

(Received 3 January 2008; accepted 21 March 2008; published online 28 April 2008)

The effect of a structure of a fullerene derivative on electronic properties of poly(3-hexylthiophene)/fullerene composite was studied at 3 cm wave band EPR in wide (77–320 K) temperature region. All the systems with different fullerene derivatives demonstrate sum spectrum of small polarons with different mobilities and contributions depending on the structure of the fullerene derivative. Both the spin-lattice and spin-spin relaxation times were determined separately by using the steady-state saturation method. The treatment of polymer matrix by fullerene derivative changes its dimensionality and conformation. This leads to the change in the spin relaxation and susceptibility as well as in the rate of polaron diffusion along polymer chain. © *2008 American Institute of Physics*. [DOI: 10.1063/1.2908819]

I. INTRODUCTION

Conjugated polymers with extended π-electron systems in their main chain attract much interest from not only pure scientific viewpoints but also due to their perspective use as flexible active matrix for new electronic devices such as light emitting diodes,[1] solar cells,[2,3] and thin film field effect transistors.[4] The understanding of the basic physics underlying the electrical, thermal, and optical behavior of organic polymeric materials is essential for the optimization of devices fabricated using these materials.

Among side chain substituted polymers, the alkyl-substituted polythiophenes[5] are seen as a major milestone in the development of high-performance solution processible electronic polymer systems. Since the parent polymer, polythiophene, already tends toward backbone planarity there is a strong cooperative self-assembly of poly(3-alkylthiophenes) (P3AT) into well ordered lamellar phases.[6,7] For some applications, this behavior has the desirable effect of enhancing interchain p-orbital overlap and thereby improving the electron transport properties. Such overlapping is higher in poly(3-hexylthiophene) (P3HT) with shorter alkyl substitute that stipulates faster polaron formation and recombination in this polymer. The nature of the coupling between adjacent alkylthiophene rings in P3HT determines its optical, transport, and electronic properties. For example, the steric repulsion between the sulfur atoms and the hexyl side groups in head-to-head conformations causes torsion in the polythiophene backbone out of planarity, and hence, a decrease in the conjugation of the π-conjugated system.[8] This effect changes the electronic band structure of the polymer and leads to a novel photoluminescence and electroluminescence.[9] Head-to-tail regioregular P3HT exhibits a planar configuration, higher mobility, and a higher degree of crystallinity in the films.[10] The illumination of a polymer/fullerene film by light leads to the photoinduced electron transfer from polymer chain to fullerene molecule and, therefore, to simultaneous formation of additional polarons P^+ and fullerene ion-radical C_{60}^{-} in the film. The efficiency of such process including the charge separation, quantum yield, the absence of the electron traps, etc., should be governed by the structure of both the polymer and fullerene derivative. P3HT and fullerene derivatives are frequently used as effective donor and acceptor composite materials in plastic solar cells.[11–13] Undoubtedly, the charge transfer in the initial and fullerene-treated polymers should be first studied before its use as active matrix of solar cells. However, the physics processes being in these systems are only scarcely studied and understood.

Polarons stabilized in P3AT possess spin $\frac{1}{2}$, so the electron paramagnetic resonance (EPR) is the powerful method for the study of such solids.[14–16] As in the case of other organic solids, the method allows one to determine main magnetic resonance parameters through the measurement of paramagnetic susceptibility, g-factor, linewidth, and line shape of the polarons and new important information on amplitude and correlation time of inside fluctuating fields in fullerene-modified P3AT compounds from longitudinal T_1 and transversal T_2 electron spin relaxation times. Spin-spin relaxation time is usually measured from the EPR linewidth, however, inhomogeneous broadening masks frequently the effect of fluctuating fields.

The main aim of this article is to clarify the role of a structure of the fullerene derivative on the magnetic, relaxation, and dynamic properties of whole spin reservoir in the polymer/fullerene system. We show the existence of polarons with different relaxations and mobilities in P3HT blended with fullerene derivatives. We studied the effective relaxation times and paramagnetic susceptibility of these paramagnetic reservoirs as well as the dynamics of mobile polarons in a wide temperature range and analyzed the effect of the dipole-dipole interaction between mobile and localized spins on these parameters. Finally, the correlation between

---

[a] Author to whom any correspondence should be addressed. Electronic mail: kivi@cat.icp.ac.ru.

the electronic and macromolecular properties is analyzed. Small polarons are formed in the initial and fullerene-modified P3HT, whose magnetic and electronic properties are governed by a structure of the fullerene derivative. The dimensionality of the polymer/fullerene system is also determined by a structure of the fullerene derivative.

II. EXPERIMENTAL

Regioregular P3HT (the chemical structure is shown in Fig. 1) with the lattice constants[7] $a=1.680$ nm, $b=0.766$ nm, and $c=0.770$ nm was purchased from Aldrich® and used without further purification. The synthesis of the soluble fullerene derivatives 1–6, was described in details previously.[17] The chlorobenzene solution of P3HT and appropriate fullerene derivatives 1–6 (1: wt. ratio) with concentration ~1 wt % was placed onto ceramic plane and dried, so that the respective composites P3HT/1, P3HT/2, P3HT/3, P3HT/4, P3HT/5, and P3HT/6 were formed as film with the size of ~4×8 mm^2 and thickness of ~0.1 mm.

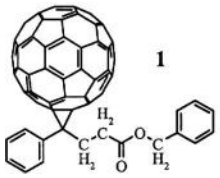

1

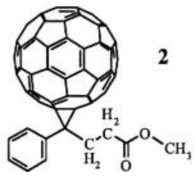

2

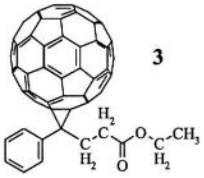

3

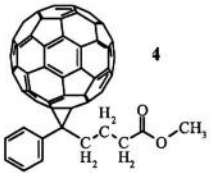

4

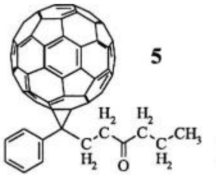

5

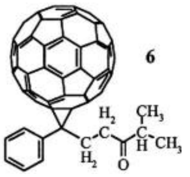

6

EPR study of these samples was performed using a 3 cm (X band, 9.7 GHz) PS-100X spectrometer with 100 kHz field ac modulation for phase-lock detection. The temperature of the sample was stabilized in nitrogen atmosphere by the BRT-IOH controller in the range of 90–320 K with the ±0.5° error. Besides, the spectra of the samples were also registered at 77 K in quartz dewar with liquid nitrogen. The total effective susceptibility of paramagnetic centers in the samples was determined by comparison of their double integrated EPR spectra with that of calibrated quantity of 1,1-diphenyl-2-picrylhydrazyl. EPR spectra were simulated using the Bruker® WINEPR SIMFONIA V.1.25 programs. The uncertainty in the determination of the peak-to-peak linewidth ΔB_{pp} and the value of g-factor was consequently $\pm 2\times 10^{-2}$ G and $\pm 2\times 10^{-4}$.

III. RESULTS AND DISCUSSIONS

A. Magnetic resonance parameters

Paramagnetic centers (PCs) in the initial P3HT sample demonstrates at 3 cm wave band EPR Lorentzian exchange-narrowed nearly symmetrical line with effective $g_{\mathrm{eff}}=2.0029$ (Fig. 1). As the sample is modified by fullerene in its spectrum appear two additional lateral lines. This fact evidences for the localization of part of polarons probably at cross bonds and/or at ends of polymer chains during such a modification. The intensity of these components decreases in the series P3HT/1→P3HT/6→P3HT/2→P3HT/3→P3HT/4→P3HT/5.

In order to determine more correctly and completely such main magnetic resonance parameters as g-tensor terms, peak-to-peak linewidth ΔB_{pp}, and paramagnetic susceptibility χ, one should model EPR spectra of PCs stabilized in the samples. We suppose that first derivative of the effective spectrum $G^{|}(B)$ of localized and mobile polarons are characterized by inhomogeneously broadened and motionally narrowed EPR spectra with Gaussian $G^{|}_{\mathrm{G}}(B)$ and Lorentzian $G^{|}_{\mathrm{L}}(B)$ distributions, respectively,[18]

$$G(B)=I_{\mathrm{G}}^{0}\frac{\sqrt{e}(B-B_0)}{\Delta B_{\mathrm{pp}}}\exp\left[-\frac{2(B-B_0)^2}{\Delta B_{\mathrm{pp}}^2}\right]+I_{\mathrm{L}}^{0}\frac{16(B-B_0)}{9\Delta B_{\mathrm{pp}}}\left[1+\frac{4(B-B_0)^2}{3\Delta B_{\mathrm{pp}}^2}\right]^{-2}. \qquad (1)$$

The deviation from g-factor for the free electron ($g_e=2.002\,32$) of the g-factor of PCs in such conjugated π-electron systems is due to noncompensated orbital momentum, which induces an additional magnetic field. The g-tensor terms are expressed by an equation[18]

$$g_{ii}=g_e\left(1+\frac{\lambda_s\rho_s(0)}{\Delta E_{nj}}\right), \qquad (2)$$

where $\rho_s(0)$ is the spin density on the sulfur nucleus, λ_s is the constant of the spin-orbit interaction of the electron spin with sulfur nucleus equal to 47 meV,[19] and ΔE_{nj} is the energy of the electron excitation from the ground orbit to nearest π^* and σ^* orbits. The orbital moment due to a direct π-π^* excitation is negligible and shows up on the neighboring C atoms only. On the other hand, the g-factor anisotropy is induced by additional fields along the x and y directions within the plane of σ skeleton and not along the perpendicular the z direction. For sulfur-containing organic solids, appropriate $\Delta E_{n\pi^*}$ and $\Delta E_{n\sigma^*}$ lie near 2.6 and 15.6 eV, respectively.[20–22] In these systems, each unpaired electron is localized on the sulfur atom, so then their isotropic g-factor lies near 2.018–2.200. Small shift of effective g-factor of the samples studied from g_e evidences that a spin is delocalized in these systems at least on two tens of sulfur sites.

Computer simulation shown that two types of PCs are indeed stabilized in the samples, namely, a polarons localized at cross bonds or/and on the short π-conjugated polymer chains R_1 with $g_{xx}=2.004\,93$, $g_{yy}=2.003\,01$, $g_{zz}=2.000\,98$,

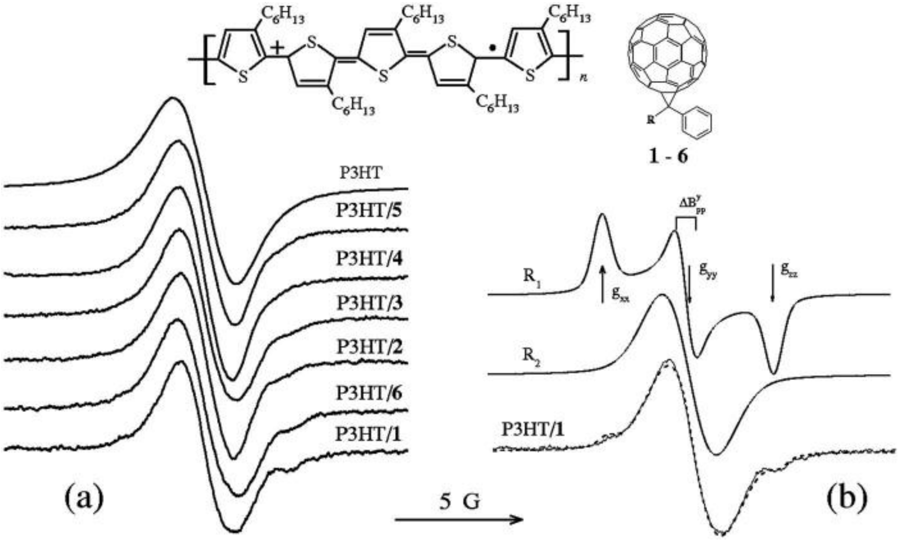

FIG. 1. (a) EPR spectra of the initial P3HT and fullerene-modified samples P3HT/1–P3HT/6 registered at 300 K and B_1=15 mG. (b) Experimental EPR spectrum of the sample P3HT/1 (solid line) compared to sum theoretical spectrum (dashed line) of localized R_1 and mobile R_2 polarons calculated from Eqs. (1) and (2) with relative concentration ratio $[R_1]/[R_2]$=0.089 and I_L^0/I_G^0=0.3 and 0.2, respectively. The formation of polaron in P3HT is shown schematically. The magnetic resonance parameters measured are shown as well.

and linewidth ΔB_{pp}=0.66 G, and a polaron moving along the main π-conjugated polymer chain R_2 with $g_{xx}=g_{yy}=g_{zz}$ =2.002 92, and ΔB_{pp}=2.15 G. The principal x axis is chosen parallel to the longest molecular c axis, the y axis lies in the thiophene rings plane, and the z axis is perpendicular to the x and y axes. The best fit of the R_1 signal was achieved using nearly Gaussian line shape, which means that the transitions are inhomogeneously broadened mainly due to unresolved hyperfine interaction of unpaired spin with protons. Simulated spectra of R_1 and R_2 PCs are shown in Fig. 1 as well. The effective g-factor of the R_1 PCs, $g_{\mathrm{eff}}=1/3\Sigma g_{ii}$, lies near to that of the R_2 ones. This fact supports the supposition made above about the nature of PCs. Spin concentration ratio $[R_1]/[R_2]$ lies near 0.089 for P3HT/1 with phenyl, the fullerene derivative's side chain, slightly decreases for P3HT/6 with more branched opposite end of the fullerene derivative's side chain and then reduces progressively for other compounds (see Fig. 1). Note, that the existence of such polarons with different relaxations and dynamics was determined by us also in other conjugated polymers.[23] This phenomenon can be explained by combined effect of the fullerene derivative's structure and conformation on the packing order of the polymer chains. Indeed, the more sphericity of the fullerene derivative, the smaller disorder of polymer chains appears. In this case, the smaller mobile polarons are localized on the polymer chains so then contributing to the R_1 spectrum.

B. Paramagnetic susceptibility

Effective spin susceptibility of the samples χ is shown in Fig. 2 as function of temperature. It is seen from the figure that this parameter depends not only on the temperature but also on the structure of a fullerene derivative. This value increases at the treating of P3HT by the fullerene derivatives 1 and 2 and then returns to the previous value in the case of the 3–6 fullerene derivatives (Fig. 2).

Generally, temperature dependent static paramagnetic

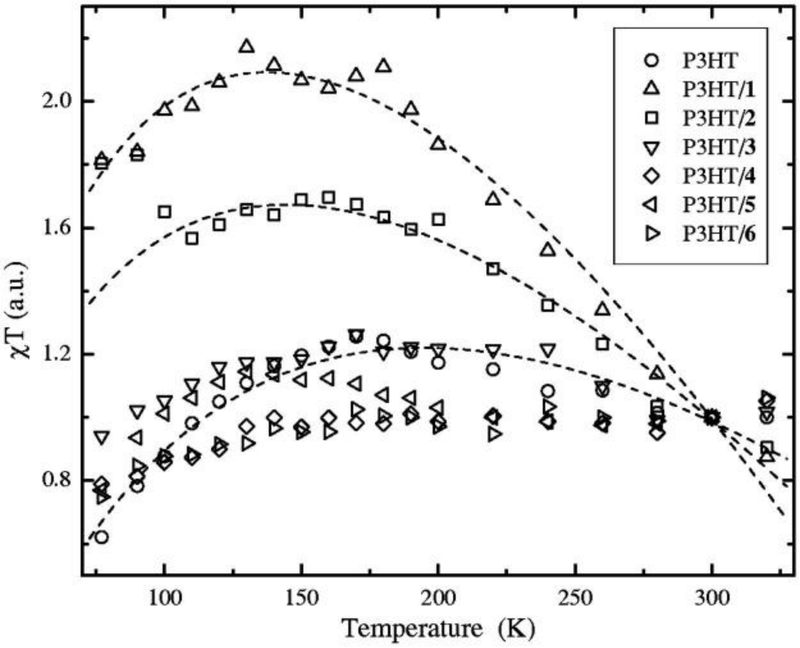

FIG. 2. χT vs T dependences obtained for the initial P3HT and fullerene-modified samples P3HT/1–P3HT/6. Top-to-down dashed lines show the dependencies calculated from Eq. (5) with E_a=2.0, 1.9, and 4.0 meV, respectively.

susceptibility of N_s localized and N_e mobile polarons with $S=\frac{1}{2}$ consists of two appropriate parts. First, contribution should follow the Curie low

$$\chi_s(T)=\frac{N_s\mu_{\text{eff}}^2}{3k_BT}, \tag{3}$$

where $\mu_{\text{eff}}=\mu_B g\sqrt{S(S+1)}$ is the effective magneton, μ_B is the Bohr magneton, and k_B is the Boltzmann constant.

The samples studied demonstrate more complex temperature dependence for own spin susceptibility (Fig. 2). The analysis shown that this value cannot be described in terms of the model proposed by Raghunathan *et al.*[24] for interacting spins in doped organic conductors, regioregular P3HT among them.[25] In order to interpret the obtained experimental data, we should consider also the term of susceptibility coming due to quasi-one-dimensional (quasi-1D) mobile polarons characterizing by midgap energy $E_g=2E_a$ near the Fermi level[26,27]

$$\chi_e(T)=2\chi_e^0\int_\Omega^\infty\frac{x}{\sqrt{x^2-\Omega^2}}\frac{e^x}{(1+e^x)^2}dx = \chi_e^0\begin{cases}\sqrt{\Omega}\exp(1-\Omega) & \text{at } \Omega\geqslant 4\\ (1-0.21\Omega^2) & \text{at } \Omega\leqslant 1/4,\end{cases} \tag{4}$$

where $\Omega=E_a/k_BT$.

The analysis shown that the E_a value evaluated using the high-temperature limit of Eq. (4) is too large (3–20 eV), so to interpret our data, we should use the other limit of Eq. (4). In this case, spin susceptibility of mobile polarons is characterized by activation low and, besides, the $T^{-1/2}$ factor appears in its temperature dependence.

Indeed, Fig. 2 shows that the experimental data obtained for all polymer systems are fitted well by the combination of Eqs. (3) and (4),

$$\chi(T)=\frac{k_1}{T}+k_2\sqrt{\frac{E_a}{k_BT}}\exp\left(1-\frac{E_a}{k_BT}\right), \tag{5}$$

with appropriate coefficients k_1 and k_2 and with E_a presented in Table I.

C. EPR linewidth

Effective EPR linewidth of PCs stabilized in the initial and fullerene-treated P3HT samples is presented in Fig. 3 as function of temperature. One can see that this value decreases distinctly at the P3HT fullerene treatment, however, changes weakly within the polymer/fullerene series. This value is mainly determined by spin-spin relaxation time T_2, however, there are several relaxation processes which cause the shortening of T_2 and hence the broadening of EPR line. One of them is the spin relaxation on the lattice phonons with a time T_1, which shortens the lifetime of a spin state and therefore broadens the line. If we represent all the other relaxation processes by the time $T_2^{|}$, we can write for effective peak-to-peak width ΔB_{pp} of a Lorentzian line[28]

TABLE I. Parameters E_a, E_{dd}, and E_b (all in meV) determined from Eq. (5), Eq. (8), and Eq. (13), respectively, as well as the D_{1D} (in 10^{11} rad/s) and $D_{\text{1D}}/D_{\text{3D}}$ values determined from Eqs. (11) and (12) at room temperature for the initial P3HT and fullerene-treated samples P3HT/1–P3HT/6 with side chains R.

Sample	R	E_a	E_{dd}	E_b	D_{1D}	D_{1D}/D_{3D}
P3HT	–	4.0	5.0	25.3	3.3	12
P3HT/**1**	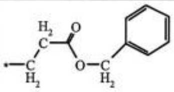	2.0	4.4	23.8	5.4	16
P3HT/**2**	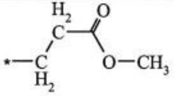	1.9	4.3	19.8	6.0	32
P3HT/**3**	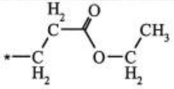	2.0	4.6	10.9	7.7	77
P3HT/**4**	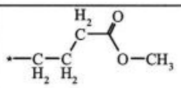	1.4	3.8	2.7	8.6	71
P3HT/**5**	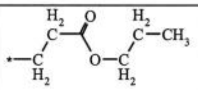	1.7	3.9	0.9	5.2	18
P3HT/**6**	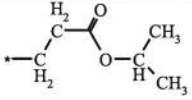	0.2	3.7	9.9	22	1300

$$\Delta B_{\text{pp}}=\frac{1}{\sqrt{3}\gamma_e}\cdot\frac{1}{T_2}=\frac{1}{\sqrt{3}\gamma_e}\cdot\left(\frac{1}{T_2^{|}}+\frac{1}{2T_1}\right), \tag{6}$$

where γ_e is the gyromagnetic ratio for electron.

For an isolated spin, there are mainly two contributions to the $1/T_2^{|}$ term of Eq. (6), namely spin dipole-dipole ω_d and hyperfine ω_h interactions.[29] However, if the spin is movable or exchange interacts with other spins with ω_{ex} exceeding both the ω_d and ω_h values its line becomes motional narrowed and[30]

$$\frac{1}{T_2}=\frac{10\omega_d^2+3\omega_h^2}{3\omega_{\text{ex}}}=\frac{\gamma_e}{3B_{\text{ex}}}[51\mu_{\text{eff}}^2n_e^2+A^2I(I+1)], \tag{7}$$

where B_{ex} is the additional magnetic field arising due to spin motion, n_e is the spin concentration, A is the hyperfine constant, and I is the nuclear spin.

The diffusing of polarons along and between chains of conjugated polymers is studied using the Bloch–Hasegawa equations.[27] The linewidth of such system spin reservoir is mainly determined by dipole-dipole activation interaction between two type of polarons with activation energy of E_{dd}, so that[27,31]

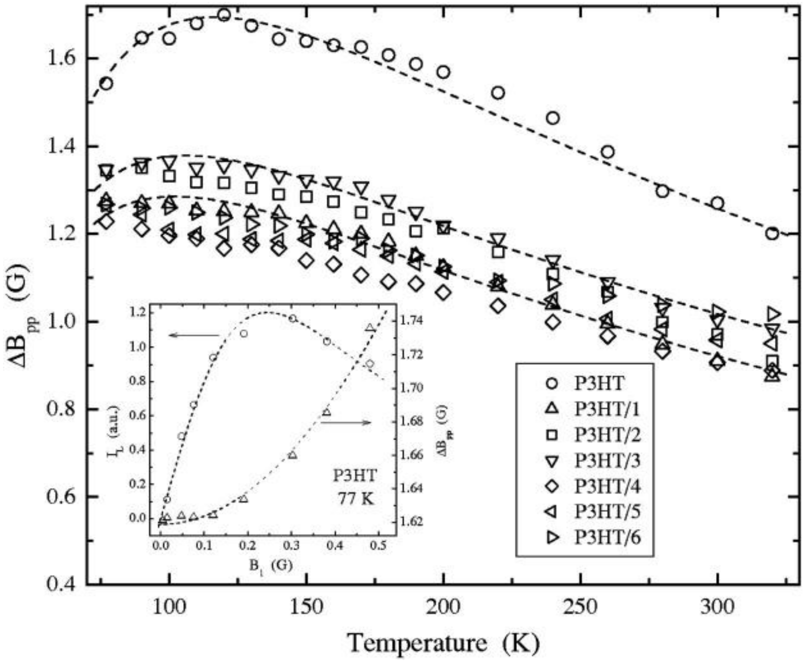

FIG. 3. Peak-to-peak linewidth of the initial P3HT and fullerene-modified samples P3HT/1–P3HT/6 as function of temperature. By the top-to-down dashed lines are shown the dependencies calculated from Eq. (8) with E_a=5.0, 4.6, 4.4 meV, respectively. In the inset, the change of the line amplitude and width of the initial P3HT sample with the B_1 value at T=77 K as well as the dependencies calculated from Eqs. (9) and (10) with $T_1=1.2\times10^{-6}$ and $T_2=4.1\times10^{-8}$ s are shown.

$$\Delta B_{\rm pp}(T) = \Delta B_{\rm pp}^0 T^{-1/2} \exp\left(-\frac{E_{\rm dd}}{k_B T}\right). \tag{8}$$

Some dependencies calculated from Eq. (8) with different $E_{\rm dd}$ values are presented in Fig. 3 as well. The figure shows that the temperature dependencies of the linewidth determined from the spectra are described well by the above equation with $E_{\rm dd}$ summarized in Table I.

D. Spin relaxation

As the magnetic term B_1 of microwave irradiation increases, the absorption line of polarons is broadened and its intensity I_L changes nonlinearly, as it is seen in Fig. 3. This happens due to the steady-state saturation of the whole spin reservoir allowing one to determine separately the effective T_1 and T_2 values from relations[32]

$$\Delta B_{\rm pp} = \Delta B_{\rm pp}^{(0)} \sqrt{1 + \gamma_e^2 B_1^2 T_1 T_2}, \tag{9}$$

$$I_{\rm L} = I_{\rm L}^0 B_1 (1 + \gamma_e^2 B_1^2 T_1 T_2)^{-3/2}, \tag{10}$$

where $\Delta B_{\rm pp}^{(0)} = \sqrt{3}/2\gamma_e T_2$ is the linewidth of unsaturated line at the $B_1 \rightarrow 0$ limit. The relaxation parameters of polarons determined from Eqs.(9) and (10) using such a method are presented in Fig. 4(a).

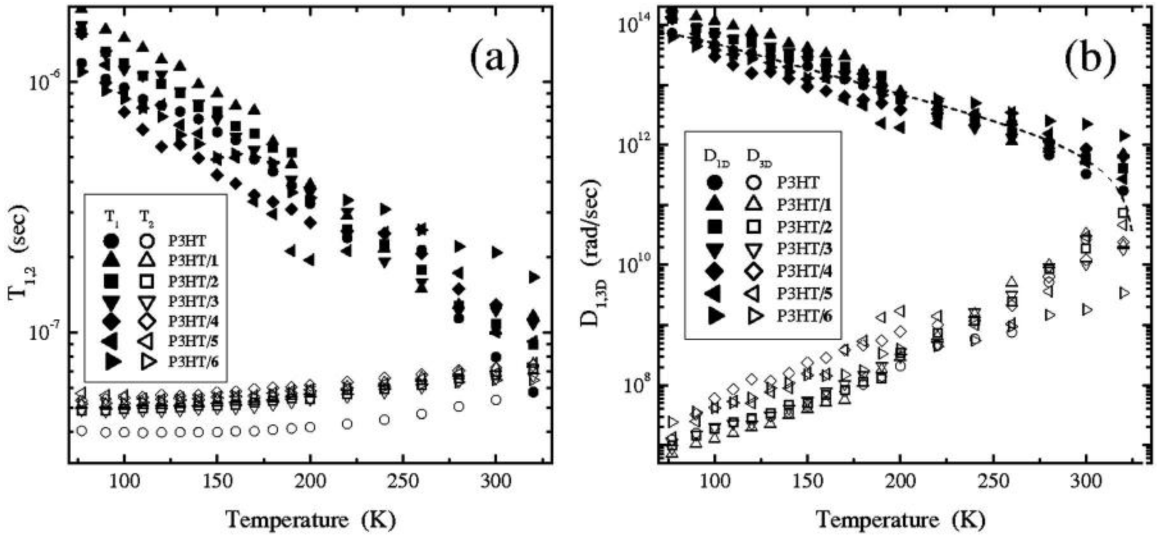

FIG. 4. Temperature dependencies of the longitudinal (T_1, filled points) and transversal (T_2, open points) relaxation times determined from Eqs. (9) and (10) (a) as well as the in-chain ($D_{\rm 1D}$, filled points) and interchain ($D_{\rm 3D}$, open points) diffusion coefficients determined from Eqs. (11) and (12) for polarons stabilized in the initial P3HT and fullerene-modified samples P3HT/1–P3HT/6. The dependence calculated from Eq. (13) with E_a=25.3 meV is shown as an example by dashed line as well.

E. Spin dynamics

A part of polarons diffusing along and between the polymer chains with respective diffusion coefficients $D_{1\mathrm{D}}$ and $D_{3\mathrm{D}}$ induces an additional magnetic field in the whereabouts of another spins that, in turn, accelerates electron relaxation of whole spin ensemble. As the relaxation times of the spins are defined mainly by their dipole-dipole interaction, the following equations can be written as:[19]

$$T_1^{-1}(\omega_e) = \langle \omega^2 \rangle [2J(\omega_e) + 8J(2\omega_e)], \tag{11}$$

$$T_2^{-1}(\omega_e) = \langle \omega^2 \rangle [3J(0) + 5J(\omega_e) + 2J(2\omega_e)], \tag{12}$$

where $\langle \omega^2 \rangle = 1/10\gamma_e^4 \hbar^2 S(S+1) n \Sigma_{ij}$ is the constant of a dipole-dipole interaction for powder with n polarons per each monomer and lattice sum Σ_{ij}, $J(\omega_e) = (2D^{|}_{1\mathrm{D}}\omega_e)^{-1/2}$ at $D^{|}_{1\mathrm{D}} \gg \omega_e \gg D_{3\mathrm{D}}$ or $J(0) = (2D^{|}_{1\mathrm{D}} D_{3\mathrm{D}})^{-1/2}$ at $D_{3\mathrm{D}} \gg \omega_e$ is a spectral density function for quasi-1D motion, $D^{|}_{1\mathrm{D}} = 4D_{1\mathrm{D}}/L^2$, ω_e is resonant angular frequency of the electron spin precession, and L is a factor of spin delocalization over a polaron equal approximately to five monomer units in P3AT.[33] The similar spectral density function was earlier used in the study of spin dynamics in other conjugated polymers.[15,23]

Figure 4(b) shows how the coefficients $D_{1\mathrm{D}}$ and $D_{3\mathrm{D}}$ of polaron diffusion in the initial and fullerene-modified samples calculated from Eqs. (11) and (12) at $L \approx 5$,[33] are changed with the temperature. The data obtained evident that the $D_{1\mathrm{D}}$ value as well as the anisotropy of spin diffusion $D_{1\mathrm{D}}/D_{3\mathrm{D}}$ tends to increase in the series P3HT → P3HT/1 → ⋯ → P3HT/6 (see Table I).

The analysis shown that the best interpretation of the $D_{1\mathrm{D}}(T)$ dependencies presented in Fig. 4 should be interpreted in terms of the motion of small polarons through activation barrier E_b in quasi-1D system.[34,35] In this case, the $D_{1\mathrm{D}}$ value should change with temperature as

$$D_{1\mathrm{D}}(T) = D_{1\mathrm{D}}^0 T^{-4} \exp\left(-\frac{E_b}{k_B T}\right). \tag{13}$$

Figure 4 evidences that the temperature dependences determined for polaron diffusion along polymer chains in the polymer systems studied are fitted well by Eq. (13) with E_b also presented in Table I. The activation barrier energies obtained lie near to those determined for lattice phonons in other conjugated polymers,[23] poly(3-octylthiophene)[36] and poly(3-hexylthiophene)[37] among them.

IV. CONCLUSION

In this work, we performed comparative EPR studies of the magnetic, relaxation, and electron dynamic properties of the initial P3HT sample and different P3HT/fullerene composites. The microwave saturation studies allowed one to determine separately all relaxation parameters of polarons with different relaxation and mobility formed in these samples. Both the effective relaxation times and paramagnetic susceptibility of polarons are governed by their dipole-dipole interaction with own microenvironment and other PCs. Spin and electronic dynamics in the P3HT can be described in terms of the activation diffusion of small polarons along the polymer chains.

The introduction of the 1–6 fullerene derivatives into polymer matrix changes its dimensionality and conformation. This changes the interaction of polarons with own microenvironment that leads to the change in their magnetic, relaxation, and dynamic parameters. The rate and anisotropy of polaronic dynamics are governed by a structure of the fullerene derivative and, probably, by its donor-acceptor properties. The data obtained show that the activation barrier E_b crossed by a polaron increases in the row P3HT/5 → P3HT/4 → P3HT/3 → P3HT/6 → P3HT/2 → P3HT/1. This is accompanied by the increase in concentration of localized polarons R_1 as well as in spin susceptibility and spin-lattice relaxation time in the polymer/fullerene system. The presence of linear side chains in the fullerene derivatives 3, 4, and 5 seems to decrease the activation barrier E_b. On the other hand, shortening (2) or branching (1 or 6) of the side chain in the molecule of the fullerene derivative results in the higher activation barrier as well as in the appearance of greater number of localized polarons on the polymer chains. This can be explained by the complex orientation and conformation effect of the fullerene side substitude (depending, e.g., on the relative position and orientation of its –CO–O– group) on a conformation of polymer chains *via* orientation and to lesser degree dispersion van der Waals forces that might change conformation of polymer chains. The interaction of polarons with other PCs characterized by the E_a and E_{dd} values is weaker then their interaction with the polymer lattice phonons characterized by E_b. The introduction of an optimal fullerene derivative leads to the simultaneous decrease of these correlated parameters and also to the acceleration of 1D polaronic diffusion in the P3HT/fullerene samples.

The dynamics of polarons photoinduced in different P3AT/fullerene systems is very interesting not only experimentally but also theoretically. We are carrying out now some deeper experimentation with P3HT and other P3AT blended with fullerene derivatives to address these questions in more detail in the future.

ACKNOWLEDGMENTS

This work was supported, in part, by the Russian Foundation for Basic Researches (Grant Nos. 05-03-33148 and 08-03-00133) and by the Human Capital Foundation (Grant No. 07-136).

[1] J. Shinar, *Organic Light Emitting Devices: A Survey* (Springer-Verlag, New York, 2002).

[2] T. Markvart and L. Castaner, *Practical Handbook of Photovoltaics, Fundamentals and Applications* (Elsevier, Oxford, 2003).

[3] C. J. Brabec, V. Dyakonov, J. Parisi, and N. S. Sariciftci, *Organic Photovoltaics: Concepts and Realization*, (Springer-Verlag, Berlin, 2003).

[4] C. D. Dimitrakopoulos and D. J. Mascaro, Org. Electron. **45**, 11 (2001).

[5] *Handbook of Conducting Polymers*, edited by T. Scotheim and J. Reynolds, 3rd edition, (CRC, Boca Raton, 2007).

[6] M. J. Winokur, D. Spiegel, Y. Kim, S. Hotta, and A. J. Heeger, Synth. Met. **28**, C419 (1989).

[7] T. J. Prosa, M. J. Winokur, J. Moulton, P. Smith, and A. J. Heeger, Macromolecules **25**, 4364 (1992).

[8] P. Barta, S. Niziol, P. Le Guennec, and A. Proń, Phys. Rev. B **50**, 3016 (1994).

[9] R. E. Gill, G. G. Malliaras, J. Wildeman, and G. Hadziioannou, Adv. Mater. (Weinheim, Ger.) **6**, 132 (1994).

[10] Z. Bao, A. Dodabalapur, and A. J. Lovinger, Appl. Phys. Lett. **69**, 4108 (1996).

[11] M. Drees, H. Hoppe, C. Winder, H. Neugebauer, N. S. Sariciftci, W. Schwinger, F. Schaffler, C. Topf, M. C. Scharber, Z. G. Zhu, and R. Gaudiana, J. Mater. Chem. **15**, 5158 (2005).

[12] M. Al Ibrahim, H. K. Roth, M. Schrödner, A. Konkin, U. Zhokhavets, G. Gobsch, P. Scharff, and S. Sensfuss, Org. Electron. **6**, 65 (2005).

[13] I. Riedel, E. von Hauff, H. Parisi, N. Martin, F. Giacalone, and V. Dyakonov, Adv. Funct. Mater. **15**, 1979 (2005).

[14] V. I. Krinichnyi, 2-mm *Wave Band EPR Spectroscopy of Condensed Systems* (CRC, Boca Raton, 1995).

[15] K. Mizoguchi and S. Kuroda, in *Handbook of Organic Conductive Molecules and Polymers*, edited by H. Nalwa (Wiley, New York, 1997), Vol. 3, Chap. 6, pp. 251–317.

[16] V. I. Krinichnyi, in *Advanced ESR Methods in Polymer Research*, edited by S. Schlick (Wiley, Hoboken, NJ, 2006), Chap. 12, pp. 307–338.

[17] J. Y. Mayorova, S. L. Nikitenko, P. A. Troshin, S. M. Peregudova, A. S. Peregudov, M. G. Kaplunov, and R. N. Lyubovskaya, Mendeleev Commun. **17**, 175 (2007).

[18] J. A. Weil, J. R. Bolton, and J. E. Wertz, *Electron Paramagnetic Resonance: Elementary Theory and Practical Applications*, 2nd ed. (Wiley-Interscience, New York, 2007).

[19] F. Carrington and A. D. McLachlan, *Introduction to Magnetic Resonance with Application to Chemistry and Chemical Physics* (Harrer & Row, Publishers, New York, Evanston, London, 1967).

[20] T. S. Cameron, R. C. Haddon, S. M. Mattar, S. Parsons, J. Passmore, and A. P. Ramirez, J. Chem. Soc. Dalton Trans. **9**, 1563 (1992).

[21] H. Bock, P. Rittmeyer, A. Krebs, K. Schultz, J. Voss, and B. Kopke, Phosphorus Sulfur **19**, 131 (1984).

[22] V. I. Krinichnyi, H.-K. Roth, and M. Schrödner, Appl. Magn. Reson. **23**, 1 (2002).

[23] V. I. Krinichnyi, Synth. Met. **108**, 173 (2000).

[24] A. Raghunathan, P. K. Kahol, J. C. Ho, Y. Y. Chen, Y. D. Yao, Y. S. Lin, and B. Wessling, Phys. Rev. B **58**, R15955 (1998).

[25] P. K. Kahol, B. J. McCormick, A. J. Epstein, and S. S. Pandey, Synth. Met. **135**, 343 (2003).

[26] D. C. Jonston, Phys. Rev. Lett. **52**, 2049 (1984).

[27] S. E. Barnes, Adv. Phys. **30**, 801 (1981).

[28] J. E. Wertz and J. R. Bolton, *Electron Spin Resonance: Elementary Theory and Practical Applications* (Chapman and Hall, London, 1986).

[29] S. A. Altshuler and B. M. Kozirev, *Electron Paramagnetic Resonance* (Academic, New York, 1964).

[30] R. Kubo and K. Tomita, J. Phys. Soc. Jpn. **9**, 888 (1954).

[31] V. A. Atsarkin and V. V. Demidov, J. Exp. Theor. Phys. **86**, 572 (1998).

[32] Ch. P. Poole, *Electron Spin Resonance, A Comprehensive Treatise on Experimental Techniques* (Wiley, New York, 1983).

[33] F. Devreux, F. Genoud, M. Nechtschein, and B. Villeret, in *Electronic Properties of Conjugated Polymers*, edited by H. Kuzmany, M. Mehring, and S. Roth (Springer-Verlag, Berlin, 1987), Vol. 76, pp. 270–276.

[34] A. R. Long, Adv. Phys. **31**, 553 (1982).

[35] J. Patzsch and H. Gruber, in *Electronic Properties of Polymers*, edited by H. Kuzmany, M. Mehring, and S. Roth (Springer-Verlag, Berlin, 1992), Vol. 107, pp. 121–124.

[36] V. I. Krinichnyi, H.-K. Roth, and A. L. Konkin, Physica B **344**, 430 (2004); V. I. Krinichnyi and H.-K. Roth, Appl. Magn. Reson. **26**, 395 (2004).

[37] Z. Chiguvare and V. Dyakonov, Phys. Rev. B **70**, 235207 (2004).